Scholar Publishing Group
Frontiers in Ocean Engineering
https://doi.org/10.38007/FOE.2020.010404
ISSN 2790-2706 Vol. 1, Issue 4: 26-34

Deformity Wave Focusing in Ocean Engineering Based on High-order Spectrum

Manojiun Kautish*

Philippine Christian University Center for International Education, Philippines

**corresponding author*

Keywords: Higher-order Spectral Model, Ocean Engineering, Deformed Wave Focusing, Wave Kurtosis

Abstract: With the increase of offshore development activities, there are more and more reports on the destruction of offshore platforms and shipwrecks caused by deformed waves. Deformed waves have the characteristics of strong destructiveness and frequent occurrence, and often appear in open seas without warning, which poses a great threat to the safety of offshore structures and marine personnel. Therefore, this paper is based on high-order spectrum(HOS). Focus on research. This paper first briefly describes the basic concepts of deformed waves and kurtosis, followed by the construction and verification of the high-order spectral numerical model and the analysis of the relationship between the peak value and the occurrence probability of deformed waves. The variation law of the focus position and the peak value of vertical wave force are analyzed and studied.

1. Introduction

With the increase of a series of marine activities such as the exploration and development of mineral oil and gas resources, the cases of marine engineering equipment, offshore structures, offshore operation ships and ocean-going passenger ships encountering harsh marine environments and extreme wave loads have increased significantly [1]. Deformed waves with large wave heights and strong nonlinear characteristics can damage or destroy marine equipment or large ships, causing huge property losses and even seriously endangering life safety [2]. In-depth study of deformed waves can avoid the damage and loss caused by extreme sea conditions, which is of great guiding significance for promoting the sustainable development of marine energy resources [3-4].

At present, many experts and scholars have carried out research on HOS and deformed wave focusing, and have achieved fruitful research results. For example, researchers such as Margus used algebraic methods to study the higher-order modified KdV equation. In the context of the Jacobi

elliptic function, they obtained the allowable eigenvalues and corresponding aperiodic eigenfunctions of the spectral problem in the higher-order model. (DT) derived solutions for rogue dn- and cn-periodic waves, and finally analyzed the nonlinear dynamics of the two rogue periodic waves [5]. Researchers such as Nnonyelu C J proposed an efficient scheme to generate quadrature compression of high-order sideband spectra in optomechanical systems by embedding second-order nonlinearities into optomechanical cavities driven by strong control fields and weak probe pulses, via Experiments demonstrate that controlling the field's second-order nonlinear strength and frequency detuning can modify the magnitude of the higher-order sidebands and improve the amount of spectral compression of the higher-order sidebands, and that higher-order sidebands can be achieved in the presence of strong second-order nonlinearities. Optimized Orthogonal Compression with Spectrum [6]. Although there are many researches on HOS and deformed wave focusing, the research on deformed-wave focusing based on HOS in marine engineering is relatively rare[7-8].

This paper studies and analyzes the focusing of deformed waves in ocean engineering based on the HOS. Therefore, the structure of this paper can be divided into three parts: the first part is an overview of the relevant theories. These two basic concepts are explained; the second part is the construction of the numerical model, and the second part is divided into three subsections: high-order spectral method, the relationship between kurtosis and deformity wave occurrence probability, and numerical model verification; the third part is about Deformed wave focusing analysis part, which mainly studies and analyzes the variation law of slamming load with focusing position and the peak value of vertical wave force.

2. Related Theories

2.1. Malformed Wave

The occurrence of malformed waves is random and accidental, and the time and place of occurrence are difficult to predict [9]. With the increase of deformed wave events, the prediction and early warning of extreme sea conditions and extreme waves have attracted more and more attention and attention of scholars, and the prediction and early warning of extreme sea conditions and extreme waves cannot be separated from the statistical characteristics of deformed waves [10-11]. According to the different wave fields studied, the statistical characteristics of deformed waves are mainly divided into the following aspects: one-way single-peak spectral random wave train, one-way double-peak spectral random wave train, and multi-directional random wave train [12]. The research methods of deformed waves include: theoretical research, field observation, physical experiment and numerical calculation. Compared with the first two research methods, the two methods of physical test and numerical calculation are economical and convenient, and are the main methods used in the research on the propagation evolution and nonlinear statistical characteristics of deformed waves at present [13-14].

2.2. Kurtosis

The size of wave kurtosis is an important indicator to study the generation probability of deformed waves, which is defined as follows:

$$K = \frac{\left\langle \left(\eta - \langle \eta \rangle\right)^4 \right\rangle}{\sigma^4} \tag{1}$$

In formula (1), σ is the standard deviation of η.

Kurtosis is a characteristic parameter that characterizes the degree of deviation between the wave height and the Gaussian distribution, and can describe the steepness of the wave height probability density function distribution shape [15]. When the wave distribution is a Gaussian distribution, the kurtosis value is equal to 3.0, and the wave height probability density function distribution is flat; for strong nonlinear waves, the kurtosis value is greater than 3.0, and the wave height probability density function distribution is steeper than the Gaussian distribution [16-17] . In addition, the larger the kurtosis value, the steeper the probability density function distribution of wave height, and the greater the probability of the occurrence of deformed waves [18].

3. Numerical Model Construction

3.1. Higher-Order Spectral Methods

In the solution process of the vertical velocity at the precise free surface position, the perturbation expansion of the velocity potential is:

$$S\ （x,z,t)=\sum_{n=1}^{N}S^{(n)}(x,z,t) \tag{2}$$

The vertical velocity is written as:

$$\frac{\partial S}{\partial z}=V(x,t)=\sum_{n=1}^{N}V^{(n)}(x,t) \tag{3}$$

where M represents the nonlinear order. For the velocity potential S, perform Taylor expansion at z=0, and combine with the free surface velocity potential to sort according to the n order, and g is the wave number, we can obtain the following form

$$S^{(1)}(x,0,t)=S^{(f)}(x,t) \tag{4}$$

$$S^{(n)}(x,0,t)=-\sum_{g=1}^{n-1}\frac{\eta^{g}}{g!}\frac{\partial^{g}}{\partial z^{g}}S^{(n-g)}(x,0,t),n>1 \tag{5}$$

3.2. The Relationship between Kurtosis and the Occurrence Probability of Deformed Wave

We take the kurtosis value and the probability of occurrence of deformed waves obtained by statistics at different positions in the wave condition, each result is a point in the figure, the abscissa is the kurtosis value, and the ordinate is the probability of occurrence of deformed waves. It can be seen from Figure 1 that the distribution of points in the scatter diagram in Figure 1 is relatively concentrated, indicating that the probability of occurrence of deformed waves increases with the

increase of kurtosis. This may be because the third-order nonlinear effect of waves increases the probability of occurrence of deformed waves.

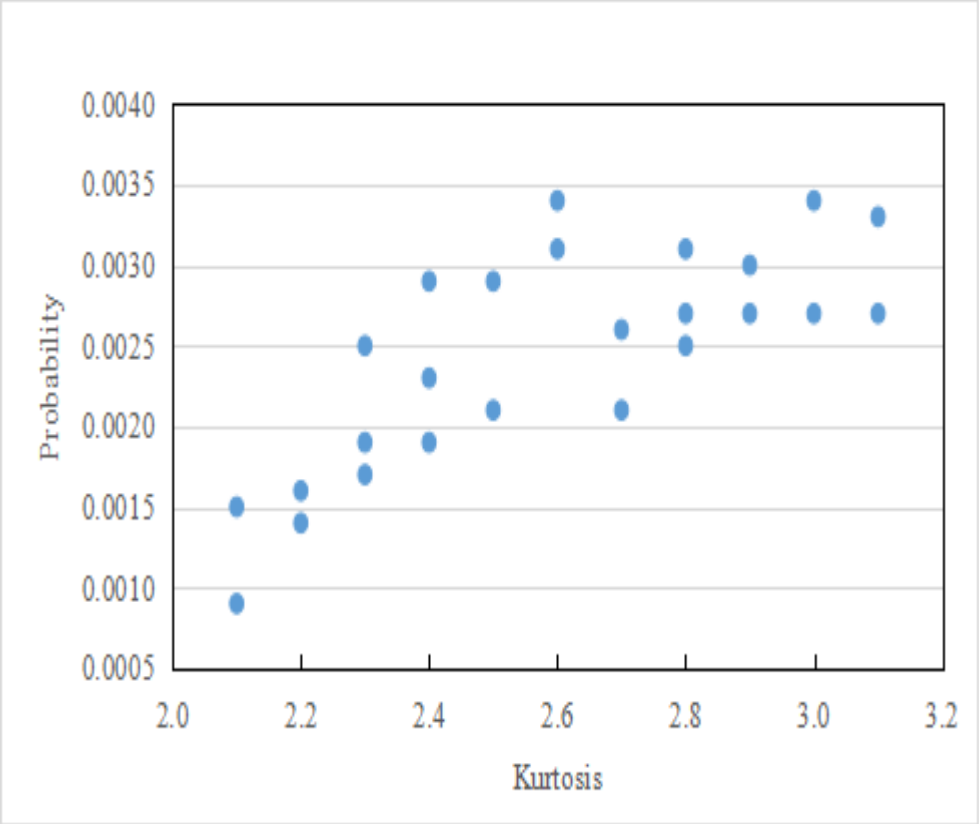

Figure 1. The relationship between the kurtosis value and the probability of occurrence of deformed wave

3.3. Numerical Model Verification

In order to ensure that the high-order spectral numerical calculation model established in this paper can accurately simulate the random wave train, Figure 2 shows the comparison between the spectrum of the numerical calculation result at the position of X=3 and the input target spectrum, and the numerical model is given in the linear case. (M=1) The spectrum of the result of the calculation.

It can be seen from Figure 2 that for the linear case (M=1), the spectrum of the numerical calculation result completely coincides with the input target spectrum, which shows that the established numerical calculation model of the higher-order spectrum can accurately simulate the linear irregular wave train. For the nonlinear case (M=5), the spectrum of the numerical calculation result is consistent with the overall trend of the input target spectrum, but there is a slight difference between 0.6 and 1.4 in the high-frequency part, this is because when M=5, the high-order The velocity potential in the spectral numerical calculation model is expanded to the fifth-order term, which is caused by considering the influence of the higher-order nonlinear term in the numerical simulation calculation process. Therefore, the numerical calculation model of HOS established in this paper can be used to simulate random wave trains and can capture the wavefront data more accurately.

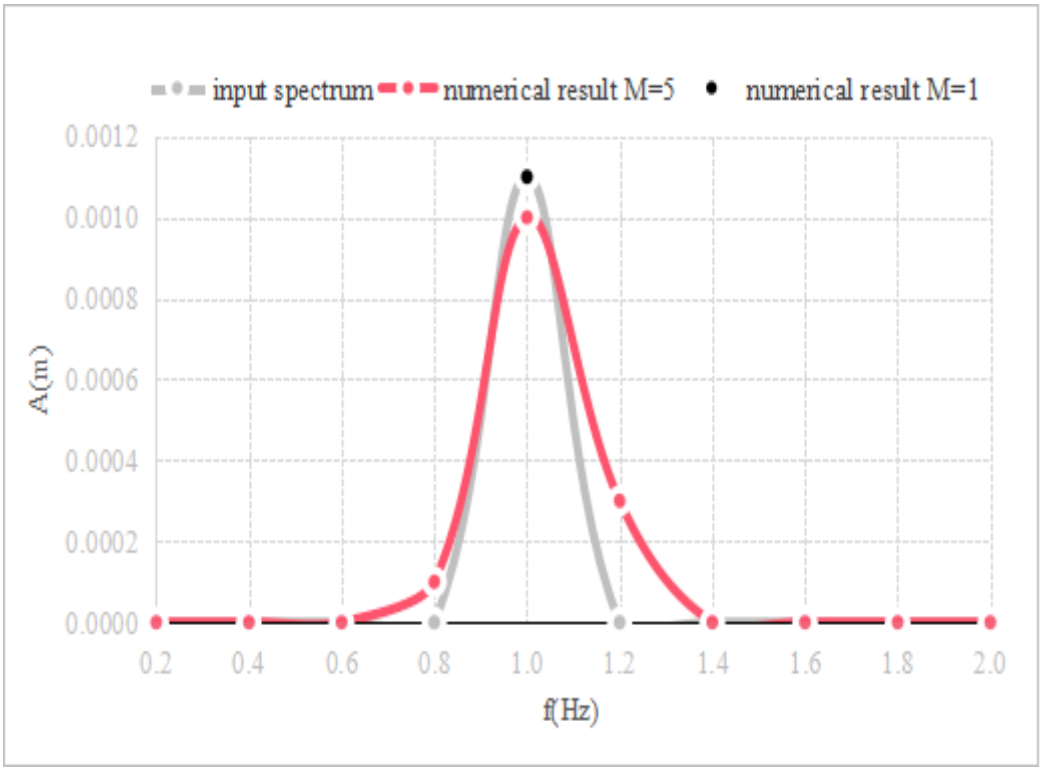

Figure 2. Comparison between the spectrum of the numerical calculation result at X=3m and the input target spectrum

4. Deformed Wave Focusing Analysis

4.1. Analysis of the Variation Law of Slamming Load with Focus Position

This section mainly studies the variation law of the slamming load at the bottom of the plate with the focusing position of the focused deformed wave. A total of 8 different focusing positions of the deformed wave are selected. Bottom, position 3 is 9m from the front of the pool. Parameter setting: the height of the air gap is 0.24m, the length of the plate is 1.1m, and the height of the wave crest is 0.17m.

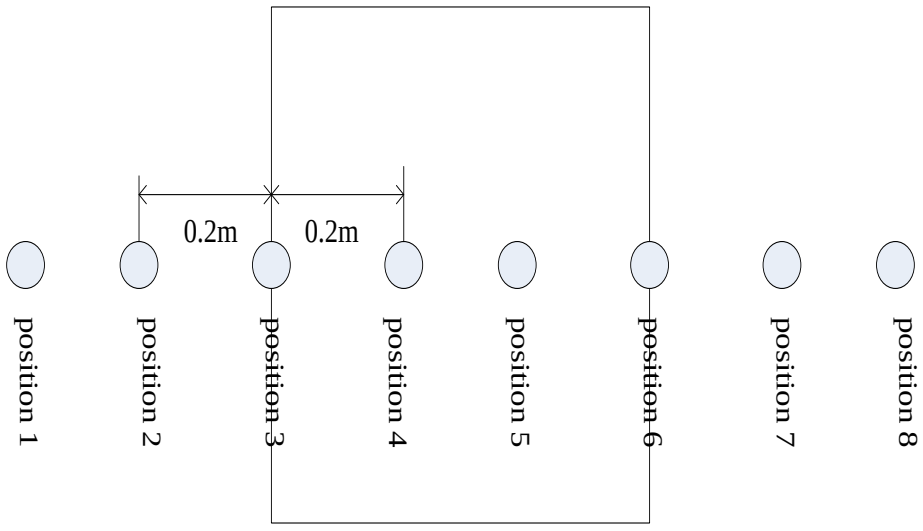

Figure 3. The distribution map of the focal position of the deformed wave

Table 1. Data table of maximum pressure values and pressure values for different focus positions

Focus position number	1	2	3	4	5	6	7	8
Fz_{max}(N)	112	131	169	145	153	163	78	62
P_{max}(Kpa)	1.8	2.3	3.6	3.2	2.7	3.3	1.4	1.3

Table 1 is the data table of the maximum slamming pressure and pressure at the bottom of the plate at different focus positions. As can be seen from the table, the maximum pressure values of the attack at positions 1 to 8 are 112, 131, 169, 145, 153, 163, 78, 62, respectively, and the maximum pressure values are 1.8, 2.3, 3.6, 3.2, 2.7, 3.3, 1.4 , 1.3. It can be seen from the table that the maximum pressure value and the maximum pressure value show an increasing trend from position 1 to position 3, and there is a downward trend from position 6 to position 8. When the focus position is position 3, the maximum pressure value and the maximum pressure value show an increasing trend. The maximum pressure value reached the highest, and the slamming maximum pressure value and maximum pressure value at position 6 ranked second. The reasons for the data changes in the table are described in detail below.

When the deformed wave is generated at the focus positions 7 and 8, the maximum pressure value and the maximum pressure value of the slamming reach the minimum, this is because the positions 7 and 8 are a certain distance from the rear end of the plate, when the wave acts on the plate, the deformed wave It has not been completely generated; although positions 1 and 2 are also a certain distance from the plate, the deformed wave has been generated in advance. When it is transmitted to the position of the plate, the attenuation of the peak of the deformed wave is not large, so the slamming pressure value is not large. decrease in magnitude. It can also be seen from the table that when the focal position of the deformed wave is located at position 3 and position 6, the maximum negative pressure value is significantly larger than other conditions. When it is generated at position 3 and position 6, compared with positions 1, 2, 7 and 8, there are more water bodies entering the bottom of the flat plate. Compared with positions 4 and 5, the water body carried by the wave crest is more hindered by the flat plate. At this time, the water body entering the bottom is caused by wave breaking, rolling and sputtering and other phenomena. The water passing through the bottom of the plate will decrease. To sum up, when the focal positions of the deformed wave are 3 and 6, the water body detached from the bottom of the plate is more than other focusing positions, and the negative pressure value and pressure value generated are also greater than other focusing positions.

4.2. Peak Vertical Wave Force

The vertical wave force peak value of deformed wave is processed according to dimensional analysis. Fig. 4 is a graph showing the relationship between the peak value of the vertical sub-wave force and the scattering parameters with different wave amplitudes. It can be seen from the figure that when the wave amplitude is 0.06 and 0.07, the peak value of vertical wave force shows a decreasing trend as a whole with the increase of scattering parameters. The increase of λ is unchanged at first and then decreases, but the decrease of the four amplitude peaks is not large, which reflects that the change of the wavelength parameter has a small effect on the vertical wave force. Different wave amplitude peaks in Figure 4 are different. When the wave amplitude is 0.02, 0.04, 0.06, and 0.07, the order of the peak values is 0.02<0.04<0.06<0.07, which shows that the abnormal wave amplitude has a positive correlation with the peak value of the vertical wave force. , with the increase of the amplitude, the peak shows an increasing change.

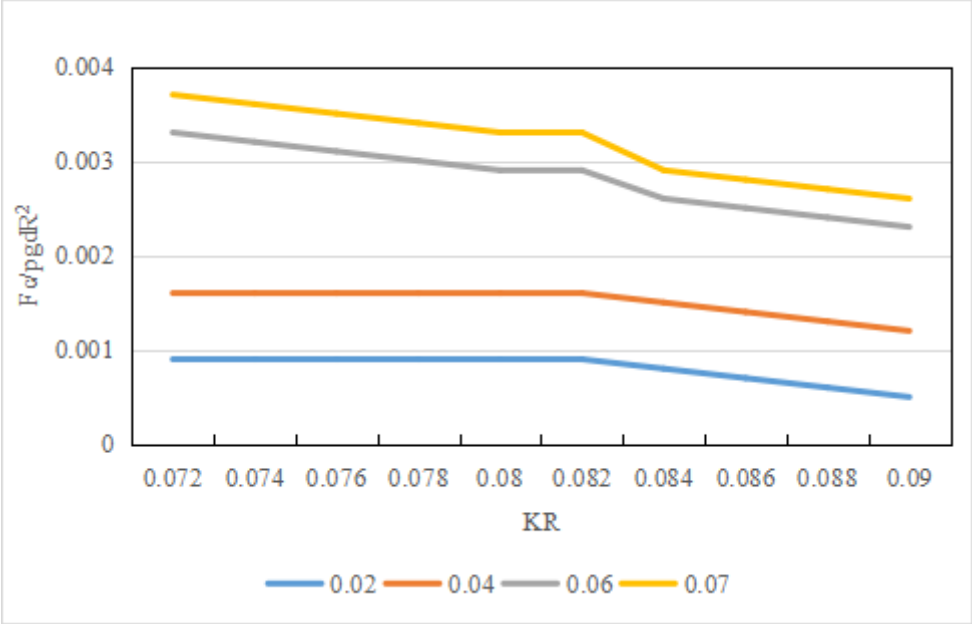

Figure 4. Relationship between the peak value of deformed wave and scattering parameters under different wave amplitudes

Figure 5 shows the relationship between the vertical dimensionless wave force peak and wave steepness. The Tp values in the figure are 1.0041, 1.0394, and 1.1101 in turn. It can be seen from the figure that under the same Tp value, with the increase of wave steepness, the vertical wave force peak value of deformed wave shows a trend of first slightly increasing and then decreasing, that is, with the continuous increase of wave steepness, the vertical wave force There is a maximum value. Under different Tp values, the peak value of vertical wave force of deformed wave increases with the increase of Tp value. It needs to be pointed out here that when the amplitude is 0.05 meters in this numerical calculation, the wave breaks slightly before the focusing position, and when the amplitude is 0.06 meters, the wave breaks obviously before the focusing position. Wave force peaks have an impact.

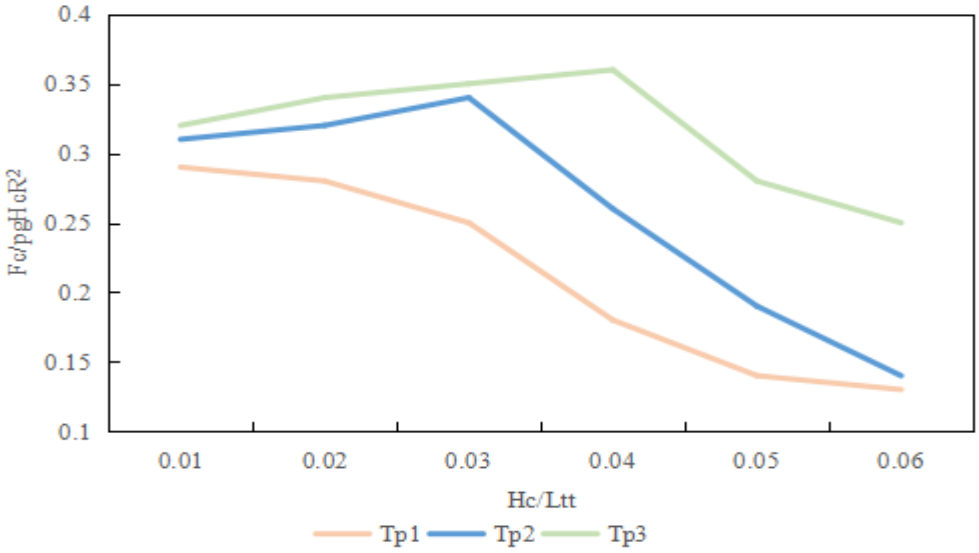

Figure 5. The relationship between the peak value of the deformed wave and the wave steepness under different Tp

5. Conclusion

The research on the focusing of deformed waves based on the HOS is beneficial to the development of marine engineering. Therefore, this paper studies and analyzes the focusing of deformed waves in marine engineering based on the HOS. Through the research, this paper draws the following conclusions: the larger the kurtosis value of the wave surface, the higher the probability of deformed waves; the numerical calculation model of the HOS can be used to simulate the random wave train, and can capture the wave surface data more accurately; The analysis of the variation law of the slamming load with the focusing position shows that when the focal position of the deformed wave is at the bottom of the plate, the water body detached from the bottom of the plate is more than other focusing positions, and the negative pressure value and pressure value generated are also larger than other focusing positions; wavelength parameter The change of the vertical wave force has little effect on the vertical wave force; under the same Tp value, with the increase of the wave steepness, the vertical wave force peak value of the deformed wave shows a trend of first slightly increasing and then decreasing; Influence on wave force peaks. There are many deficiencies in this paper, which need to be improved, but it is worth continuing to study the monstrosity focusing based on the HOS.

Funding

This article is not supported by any foundation.

Data Availability

Data sharing is not applicable to this article as no new data were created or analysed in this study.

Conflict of Interest

The author states that this article has no conflict of interest.

References

[1] Lam C T , Ng B K . Fast Spectrum Sensing Using Spatial Higher Order Statistics With Large Receive Antenna Array. IEEE Communications Letters, 2019, 23(6):1061-1064. https://doi.org/10.1109/LCOMM.2019.2909882

[2] Mousumi, Haque, Yosuke, et al. Spectrum Sensing Based on Higher Order Statistics for OFDM Systems over Multipath Fading Channels in Cognitive Radio. Journal of Signal Processing, 2019, 23(6):257-266. https://doi.org/10.2299/jsp.23.257

[3] Ewans K , Christou M , Ilic S , et al. Identifying Higher-Order Interactions in Wave Time-Series. Journal of Offshore Mechanics and Arctic Engineering, 2020, 143(2):1-18. https://doi.org/10.1115/1.4047930

[4] Koch J , Li S , Pachnicke S . Transmission of Higher Order Solitons Created by Optical Multiplexing. Journal of Lightwave Technology, 2019, 37(3):933-941. https://doi.org/10.1109/JLT.2018.2883826

[5] Margus, Rtsep, Juha, et al. Higher Order Vibronic Sidebands of Chlorophyll a and Bacteriochlorophyll a for Enhanced Excitation Energy Transfer and Light Harvesting.. The journal of physical chemistry. B, 2019, 123(33):7149-7156. https://doi.org/10.1021/acs.jpcb.9b06843

[6] Nnonyelu C J , Wong K T , Lee C H . Higher-order figure-8 sensors in a pair, skewed and collocated—Their azimuthal "spatial matched filter" beam-pattern. The Journal of the Acoustical Society of America, 2020, 147(2):1195-1206. https://doi.org/10.1121/10.0000579

[7] Volyar A V , Bretsko M V , Akimova Y E , et al. Avalanche instability of the orbital angular momentum higher order optical vortices. Computer Optics, 2019, 43(1):14-24. https://doi.org/10.18287/2412-6179-2019-43-1-14-24

[8] Gabr M M , El-Desouky B , Shiha F , et al. Higher Order Moments, Spectral and Bispectral Density Functions for INAR(1). International Journal of Computer Applications, 2018, 182(9):1-12. https://doi.org/10.5120/ijca2018917686

[9] Poornima R , Basha A M . Efficient Detection of Signal in MIMO System Using Modified Memetic Algorithm with Higher Order QAM Constellations. Applied Mathematics & Information Sciences, 2018, 12(3):665-671. https://doi.org/10.18576/amis/120323

[10] Kim K , Yoo S , Kang S , et al. Mortality of Children with Autism Spectrum Disorder Using Data from a Large-Scale Korean National Cohort.. Yonsei medical journal, 2020, 62(10):943-947.

[11] Moniz D , Pedro J , Pires J . Network design framework to optimally provision services using higher-symbol rate line interfaces. Optical Communications and Networking, IEEE/OSA Journal of, 2019, 11(2):174-185. https://doi.org/10.1364/JOCN.11.00A174

[12] Ro A , Ksab C , Jma B , et al. Abnormal cortical activation during silent reading in adolescents with autism spectrum disorder. Brain and Development, 2019, 41(3):234-244. https://doi.org/10.1016/j.braindev.2018.10.013

[13] Kataka E , Walingo T . Energy efficient statistical cooperative spectrum sensing in cognitive radio networks. Saiee Africa Research Journal, 2018, 109(1):36-47. https://doi.org/10.23919/SAIEE.2018.8531798

[14] Garg M . A Note on the Higher–order Nonlinearity of Niho Function. Fundamenta Informaticae, 2018, 162(1):37-42. https://doi.org/10.3233/FI-2018-1712

[15] Glennie A . Adam Constable (ed), Keating on Offshore Construction and Marine Engineering Contracts. Edinburgh Law Review, 2020, 24(1):153-154. https://doi.org/10.3366/elr.2020.0614

[16] Northardt T . Case study of the higher-order ambiguity function applied to array element signal estimation for non-linear sensor array fault resiliency. Radar, Sonar & Navigation, IET, 2019, 13(10):1850-1856. https://doi.org/10.1049/iet-rsn.2018.5083

[17] H Boukamcha, M Atri, F Smach. A real-time auto calibration technique for stereo camera. International Journal of Computer Aided Engineering and Technology, 2020, 12(1):74-94. https://doi.org/10.1504/IJCAET.2020.103841

[18] Dubrovskyi R . The Psycholinguistic Portrait of the Traitor in Ukrainian Artistic Military Prose of the Second Half of the XX Century. PSYCHOLINGUISTICS, 2020, 27(2):113-136. https://doi.org/10.31470/2309-1797-2020-27-2-113-136